Liquid Crystals
Publication details, including instructions for authors and subscription information:
http://www.informaworld.com/smpp/title~content=t713926090

Potential infrared liquid crystals

Shin-Tson Wu[a]; Robert J. Cox[b]
[a] Hughes Research Laboratories, Malibu, California, U.S.A. [b] IBM Almaden Research Center, San Jose, California, U.S.A.

To cite this Article Wu, Shin-Tson and Cox, Robert J.(1989) 'Potential infrared liquid crystals', Liquid Crystals, 5: 5, 1415 — 1424
To link to this Article: DOI: 10.1080/02678298908027779
URL: http://dx.doi.org/10.1080/02678298908027779

LIQUID CRYSTALS, 1989, VOL. 5, NO. 5, 1415–1424

Potential infrared liquid crystals

by SHIN-TSON WU
Hughes Research Laboratories, 3011 Malibu Canyon Road, Malibu, California 90265, U.S.A.

and ROBERT J. COX
IBM Almaden Research Center, 650 Harry Road, San Jose, California 95120-6099, U.S.A.

Principles for selecting potential infrared nematic liquid crystals are described. Optical and electro-optic properties of two cyanotolanes, 4-*n*-alkyl-4′-cyanotolanes and three commercial liquid-crystal mixtures were chosen for evaluation. Their applications for modulating infrared radiation are addressed.

1. Introduction

Since the discovery of unusually high birefingence in some nematic liquid crystals in the infrared (I.R.) region [1, 2], several useful devices for modulating or manipulating I.R. radiation have been developed. For example, an I.R. liquid-crystal light valve (LCLV) [3] can convert visible images to I.R. (3–5 or 8–12 μm) for missile-seeker testing; a liquid-crystal optical power limiter [4, 5] can control a CO_2 laser's power passively to prevent the detector from being damaged; and a single-beam amplification by degenerate two-wave mixing in liquid crystals has been demonstrated at a wavelength of 10·6 μm [6].

For electro-optic modulation of I.R. radiation employing nematics the ideal liquid crystal should possess the following properties: (1) a high merit factor, which is defined as $K_{11}\,\Delta n^2/\gamma_1$ [7], where Δn is the I.R. birefringence and γ_1/K_{11} the viscoelastic coefficient; (2) low threshold voltage (V_{th}); (3) small absorption and scattering; (4) wide nematic range; and (5) good chemical and photo-stabilities. These desired properties may not all be satisfied by a single-component material, and the priority has to be set according to the individual application. For instance, a low threshold voltage is important for image processing using a LCLV [8, 9], but may not be so critical for an active matrix display; room-temperature operation of a liquid-crystal device is desirable but not required absolutely; small absorption and scattering improves the optical efficiency and reduces the thermal effect of the device, but as long as it is not too lossy it can be tolerated. However, high merit factor and good thermodynamic stability are hard to compromise. Without good thermodynamic stability, the lifetime of the device becomes questionable. On the other hand, a low merit factor means poor performance.

2. Principles for selecting I.R. liquid crystals

One obvious way to obtain a large merit factor $K_{11}\Delta n^2/\gamma_1$ is to find a material with both high Δn and low γ_1/K_{11}. For many liquid-crystal substances and mixtures studied to date, a high Δn is often associated with a high viscosity, and a low viscosity is often associated with a low Δn. In order to achieve both high Δn and low γ_1/K_{11}

0267-8292/89 $3.00

simultaneously, correlations between Δn, γ_1/K_{11} and liquid-crystal molecular structures need to be analysed thoroughly and materials synthesized accordingly.

Recently, some highly conjugated LC molecules

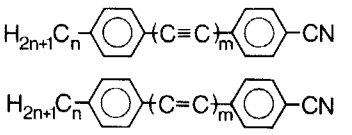

(1)

with $m = 1$, i.e. cyanotolanes and cyanostilbenes, have been found to exhibit not only high Δn but also low viscosity [10]. Furthermore, owing to the polar cyano end group, their dielectric anisotropy is large and threshold voltage is low (about $1\,V_{rms}$). Therefore, these materials are very promising for both visible and I.R. applications. In the U.V. spectral region, photostability of these molecules is a great concern because their electronic-resonance wavelengths extend to the near-visible region. However, for I.R. application, photostability of these highly conjugated molecules is assured because the major absorption in the I.R. region is due to some discrete molecular vibrational bands. Here more results on cyanotolanes (4-*n*-alkyl-4′-cyanotolanes, *n*CDP) are presented, including their optical and electro-optic properties.

Because of the limited availability of cyanotolanes and their narrow nematic ranges, some promising commercial liquid-crystal mixtures were also investigated. Among the many commercial mixtures, it is difficult to find one that possesses both high birefringence and low viscosity. A material with high Δn is often accompanied by a large γ_1/K_{11} at room temperature, and one showing low viscosity is usually coupled with a low Δn. The liquid crystals with low Δn and high γ_1/K_{11} are least attractive and will not be considered here.

The potential of low-viscosity materials for I.R. application has not yet been studied thoroughly because of their unfavourable birefringence. The merit factor is proportional to the square of Δn. Unless a liquid-crystal's advantage in γ_1/K_{11} overcomes its disadvantage in Δn^2, the merit factor of this material is not expected to be very promising.

A liquid crystal or a mixture with high Δn, although its γ_1/K_{11} may not be very attractive at room temperature, deserves special attention. Studies show that such a material has great potential for improving its merit factor at its optimal operation temperature T_{op} provided that it has a wide nematic range and high nematic–isotropic phase-transition temperature T_{NI} [7]. The T_{op} of a nematic is somewhat lower than its T_{NI} by

$$T_{op} \approx T_{NI}\left(1 - \frac{3\beta k T_{NI}}{E}\right), \tag{2}$$

where k is Boltzmann's constant, E the activation energy and β a material constant. For some biphenyl-hosted mixtures, such as E-7 and E-44 (BDH Chemicals Ltd), their T_{op} values are about 20° lower than their T_{NI} values. By operating a nematic at its T_{op}, significant improvement in the merit factor can be achieved. The reason is simple: as the temperature increases, Δn drops at a rather slow rate when T is away from T_{NI}. A more drastic change occurs as T approaches T_{NI}. However, γ_1/K_{11} declines exponentially as the temperature increases, and then gradually saturates when it approaches T_{NI}. Thus the merit factor maximizes at a temperature T_{op} that is close to T_{NI}. From this analysis, high birefringence seems to be the primary concern in

selecting a liquid crystal for electro-optic application. The low viscoelastic coefficient at room temperature is a highly desirable but not an absolutely necessary requirement, as it can always be improved by the temperature effect.

The birefringence of a LC is related to molecular properties by [2]

$$\Delta n = G \frac{\lambda^2 \lambda^{*2}}{\lambda^2 - \lambda^{*2}}, \tag{3}$$

where

$$G = gNZS(f_{\parallel}^* - f_{\perp}^*);$$

here g is a constant, N is the molecular packing density, Z is the number of active electrons (e.g. π-electrons), S is the orientational order parameter, which is temperature-dependent, and $f_{\parallel}^* - f_{\perp}^*$ is the differential oscillator strength at the mean electronic resonance wavelength λ^* [11]. λ^* depends on the detailed molecular structure, and is usually in the U.V. region. Therefore in the I.R., where $\lambda \gg \lambda^*$, Δn is reduced to

$$\Delta n \xrightarrow{\text{IR.}} G\lambda^{*2}, \tag{4}$$

which is essentially independent of wavelength except in the vicinities of the molecular vibrational bands [2]. The quadratic dependence of Δn on λ^* and the linear dependence on G provide us with useful guidelines in selecting mesogenic molecules. By increasing the π-electron conjugation length, λ^* is shifted to a longer wavelength, which is favourable in improving I.R. birefringence, according to equation (4). However, lengthening the π-bond also affects the parameter G. It should be stressed that the parameter G represents a combinational effect on N, Z, S and $f_{\parallel}^* - f_{\perp}^*$. These parameters are not independent; rather, they are interrelated. For example, adding a $-C{\equiv}C-$ bond in the middle of the biphenyl group (which becomes a tolane) will increase λ^*, Z and $f_{\parallel}^* - f_{\perp}^*$, but, on the other hand, will reduce N, the molecular packing density, owing to the longer molecular length. The order parameter of the new compound may be affected as well, owing to the change in transition temperature. Although the individual parameters contained in G are difficult to evaluate, G and λ^* can be determined easily; they can be calculated through birefringence measurements at two discrete visible wavelengths, as shown by equation (3).

3. Experimental results

3.1. *Cyanotolanes*

The syntheses of cyanotolanes (4-*n*-alkyl-4′-cyanotolanes)

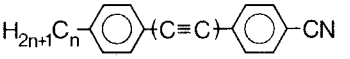

were reported more than a decade ago [12, 13]; however, their potential I.R. application has been realized only recently [10]. In [10], 5CDP was found to have not only a higher Δn but also a lower γ_1/K_{11} than for 5CB (4-*n*-pentyl-4′-cyanobiphenyl). The birefringence of 5CDP over its nematic range is about 0·27 at $\lambda = 633$ nm. Reduction in the number n of carbon atoms results in a higher packing density (see equation (3)) and, in turn, a higher Δn. We have prepared some *n*CDP with $n = 4$, 6, and 9. The 4CDP is expected to have $\Delta n \approx 0{\cdot}3$ at $\lambda = 633$ nm. The structure of 4CDP was confirmed by both carbon-13 and proton N.M.R. spectroscopy. However, these samples were found not to be pure enough, so their optical and electro-optic results are not included in the present paper. We report here some results on 6CDP and

9CDP. Although they are slightly less attractive than short-chain cyanotolanes, they do possess the basic physical properties of cyanotolanes and should be important for consideration in mixtures.

(*a*) *Transition temperature*

The transition temperatures of 6CDP and 9CDP are

$$\left.\begin{aligned} &\text{6CDP:}\quad \text{C} \xrightarrow{63^\circ\text{C}} \text{I} \xrightarrow{56{\cdot}2^\circ\text{C}} \text{N} \xrightarrow{53^\circ\text{C}} \text{C} \\ &\text{9CDP:}\quad \text{C} \xrightarrow{54^\circ\text{C}} \text{N} \xrightarrow{63{\cdot}8^\circ\text{C}} \text{I} \end{aligned}\right\} \tag{5}$$

where C, N and I represent crystal, nematic and isotropic phases respectively. The phase transition of 6CDP is monotropic and its nematic range ($53 < T < 56{\cdot}2^\circ$C) is rather narrow.

(*b*) *Optical properties*

The birefringence of 6CDP and 9CDP was measured with (i) a fixed wavelength ($\lambda = 633$ nm) but different temperature, and (ii) a constant temperature but different wavelengths. The temperature-dependent birefringence results are shown in figure 1(*a*); the dots represent experimental results at some reduced temperature, $T_R = T/T_{NI}$. The solid lines represent a fit of the experimental results using the empirical formula [14]

$$\Delta n(T) = \Delta n_0 (1 - T_R)^\beta, \tag{6}$$

where Δn_0 is the birefringence at $T_R = 0$ and β is a material parameter, the same as that in equation (2). From figure 1(*a*), [Δn_0, β] is found to be [0·372, 0·115] and [0·351, 0·139] for 6CDP and 9CDP respectively. Generally speaking, the smaller the n (carbon number), the higher the Δn_0 (i.e. a higher Δn).

From the wavelength-dependent birefringence measurements, G and λ^* of a liquid crystal can be evaluated through equation (3). The wavelengths used for our measurements were from a tunable Ar^+ laser and a HeNe laser. Equation (3) fits the experimental results very well and [G, λ^*] of each nematic are obtained as listed in the table.

Some physical properties of cyanotolanes (nCDP).

Compound	T_R	$G/10^{-6}\,\text{nm}^{-2}$	λ^*/nm	γ_1/K_{11}/ms/μm^2	V_{th}/V_{rms}
6CDP	0·991	2·41	271	10·0	1·0
9CDP	0·972	2·21	272	10·3	1·3

From this the mean electronic resonance wavelength λ^* of nCDP is found to be about 272 nm (independent of n), which is longer than that for the biphenyls ($\lambda^* \approx 248$ nm) because of the elongated π-electron conjugation length. Another tendency shown in the table is that the smaller n, the larger G. A more quantitative comparison should be made at the same reduced temperature. The larger G results from the higher packing densities for shorter-chain molecules.

The λ^* obtained can also be verified by U.V. absorption measurement [10]. In this measurement, the red shift deserves special attention. Because of the very high absorption coefficient of liquid crystals in the U.V. region, the solution method is frequently employed to measure the electronic resonance wavelengths; the results vary

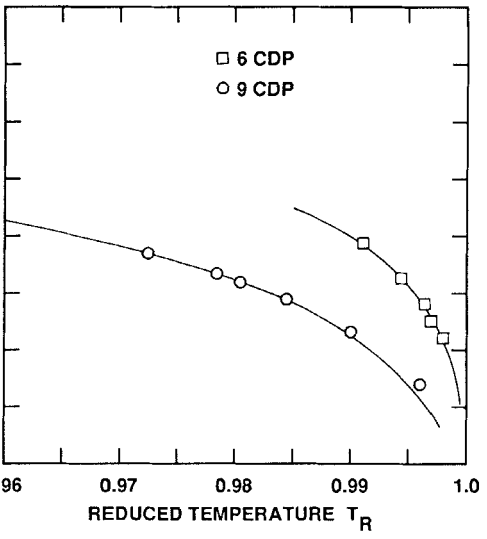

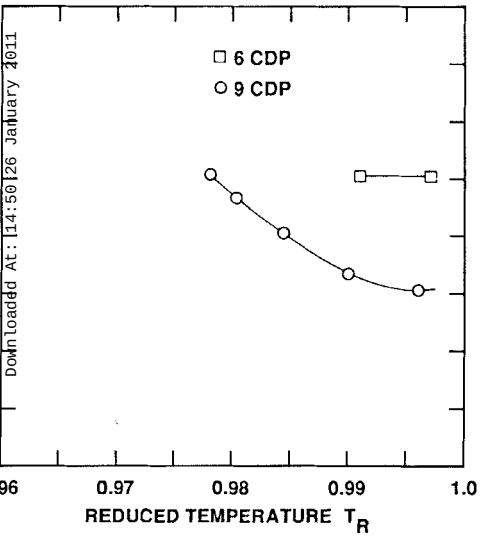

pendent birefringence (*a*) and viscoelastic coefficient (*b*) of 6CDP laser (λ = 633 nm) was used for these measurements. Solid lines in to equation (6) with parameters [Δn_0, β] = [0·372, 0·115] and DP and 9CDP respectively.

To demonstrate the solvent effect, the U.V. absorption of r three conditions: (*a*) nematic phase; (*b*) diluted solution H_3CN; and (*c*) diluted solution with a non-polar solvent, hown in figures 2 (*a*), (*b*) and (*c*) respectively. In figure 2(*a*) n), parallel-aligned liquid-crystal layer sandwiched between s used for the measurements. The use of unpolarized and (using a Glan–Thompson polarizer) does not show a dis- vithin 1 nm) in the absorption spectrum. Careful comparison (*c*) reveals a red shift in the nematic phase measurement.

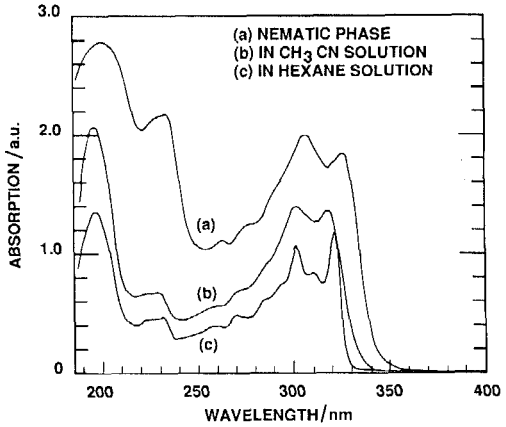

Figure 2. U.V. absorption spectra of 9CDP in (*a*) the nematic phase, (*b*) a dilute solution with a polar solvent (CH_3CN), and (*c*) a diluted solution with a non-polar solvent (hexane). A red shift in the nematic phase is observed.

In figure 2(*a*) the two longest absorption bands peak at about 306 and 326 nm. However, these two peaks shift to about 302 and 318 nm in figure 2(*b*), and about 302 and 321 nm in figure 2(*c*). In figure 2(*c*) another peak centred at about 311 nm appears. These differences are attributed to the complicated intermolecular interactions. In dilute solution in a non-polar solvent each mesogenic molecule is surrounded by many non-polar molecules. Because of the very weak interaction between this molecule and the non-polar solvent, this absorption spectrum should be very similar to that of the pure mesogenic molecules in their vapour phase [15]. However, in the nematic phase each molecule is surrounded by many identical molecules. The molecular orbitals of the conjugated π-electrons overlap slightly with their neighbours, resulting in a red shift. Although the magnitude of the red shift is only a few nanometres, this shifted spectrum represents the true absorption spectrum affecting the observed birefringence (through the λ^* effect). Unlike many liquid-crystals compounds (e.g. the cyanobiphenyls), whose absorption peaks in a polar solvent are longer than those in a non-polar solvent [15]; cyanotolanes show a reverse effect. The physical mechanism responsible for this abnormal behaviour is currently under investigation. It is worth mentioning that the U.V. absorption spectrum of *n*CDP is independent of *n*, the number of carbon atoms. This is because the absorption of those σ-electrons (C–H bonds) appears at shorter wavelengths (near 100 nm). Only π-electrons are relevant to the absorption shown in figure 2.

From the absorption spectrum shown in figure 2(*a*), λ^* of *n*CDP can be estimated. Owing to its complicated absorption spectrum, λ^* is difficult to determine accurately from the U.V. absorption. From the average of two bands (centred at about 220 and 320 nm), λ^* of *n*CDP is estimated to be about 270 nm, which is in fairly good agreement with results (see table 1) obtained by the birefringence measurement technique.

The I.R. absorption of 9CDP was measured in its isotropic state in the 2·5–50 μm region. The result is almost identical with that for 5CDP at its nematic phase, as reported in [10]. Apart from some discrete molecular vibrational bands, *n*CDP is basically transparent in the I.R. spectral region. The molecular rotational absorptions are expected to take place in the far-I.R. region ($> 100\,\mu$m). Therefore useful electro-optic application in many window regions can be obtained.

(*c*) *Electro-optic effect*

The response times and threshold voltages V_{th} of 6CDP and 9CDP were evaluated at different temperatures. From the small signal phase decay time measurement

$$\delta(t) = \delta_0 \exp(-2t/\tau_0), \tag{7}$$

τ_0 ($=\gamma_1 d^2/K_{11}\pi^2$) and γ_1/K_{11} can be obtained. δ_0 in equation (7) represents the phase change (with reference to the null-voltage state) of a parallel aligned liquid-crystal cell under an applied voltage V_0 that is just slightly above V_{th}. The temperature-dependent γ_1/K_{11} of 6CDP and 9CDP are shown in figure 1(*b*). Because of the very narrow nematic range of 6CDP, only two data points were taken. The results indicate that γ_1/K_{11} of 6CDP is in the saturation region. On the other hand, 9CDP shows a larger effect of temperature on γ_1/K_{11}. The small viscoelastic coefficient of the cyanotolanes makes these materials very attractive for electro-optic applications. The physical mechanisms responsible for the low viscoelastic coefficient of the cyanotolanes are not compeltely understood yet. The reduced γ_1/K_{11} of *n*CDP may result from (1) its relatively high nematic temperature and (2) its weak intermolecular association.

The threshold voltages of 6CDP and 9CDP were measured at 10 kHz sine-wave excitation, and the results are listed in the table. Temperature has a weak effect on V_{th}; V_{th} decreases slightly as the temperature increases. The low threshold of the cyanotolane is due to the strong dipole moment of the cyano group. In the same homologues, V_{th} varies with n. A shorter chain molecule is more polar; therefore, a lower V_{th} results.

3.2. *Commercial liquid-crystal mixtures*

Since the yield in the synthesis of cyanotolanes is low and their nematic range is narrow, some commercially available mixtures were chosen for evaluation. The major consideration is their high birefringence as discussed in §2. These mixtures were: E-7 (reference material), E-44, and RO-TN-404 (Hoffman LaRoche Chemicals). The nematic ranges of these liquid crystals are

$$\left.\begin{array}{ll} \text{E-7} & -10°\text{C} < T < 60°\text{C}, \\ \text{E-44} & -6°\text{C} < T < 100°\text{C}, \\ \text{RO-TN-404} & \sim -10°\text{C} < T < 105°\text{C}. \end{array}\right\} \tag{8}$$

The major component of these three mixtures is a cyanobiphenyl. Their λ^* values were measured to be about 250, 250 and 253 nm for E-7, E-44 and RO-T-404 respectively; these λ^* values are insensitive to temperature.

(*a*) *Electro-optic effect*

Two methods can be used to characterize the merit factor of a liquid crystal: (i) separate measurements of the temperature dependent Δn and γ_1/K_{11}, and then calculation of $K_{11}\,\Delta n^2/\gamma_1$ at each temperature; and (ii) direct measurement of $K_{11}\,\Delta n^2/\gamma_1$ by employing the recently developed transient nematic effect [16, 17]. The second method turns out to be quite simple; it involves measurement of the optical decay time (to the first minimum in the parallel-polarizer configuration) in a highly deformed ($V \gg V_{th}$) parallel-aligned cell. This decay time t_0 is inversely proportional to the merit factor:

$$t_0 \approx \left(\frac{\Delta/\pi}{2\pi}\right)^2 \frac{\gamma_1}{K_{11}\,\Delta n^2}\,\lambda^2. \tag{9}$$

where Δ is the associated phase change.

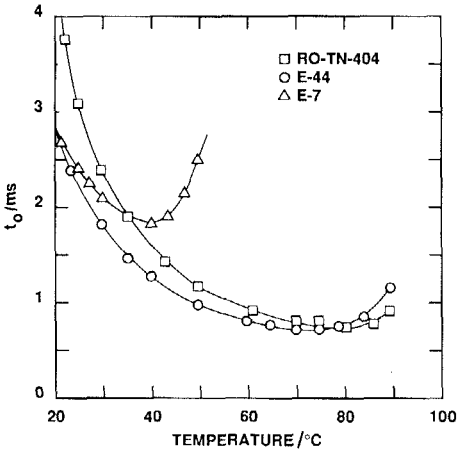

Figure 3. Temperature-dependent transient response time t_0 of three commercial liquid-crystal mixtures: E-7, E-44 and RO-TN-404. t_0 is inversely proportional to the merit factor, as described in equation (9). The laser wavelength used for these measurements was $\lambda = 633\,\text{nm}$. The T_{NI} values of these three mixtures are 60, 100 and 105°C respectively.

As we see from equation (9), this measurement is not sensitive to the liquid-crystal layer thickness and the applied voltage (as long as $V \gg V_{th}$) and it is convenient to use. Figure 3 shows experimental results for the temperature-dependent t_0 (at $\lambda = 633\,\text{nm}$) of E-7, E-44 and RO-TN-404. In the room-temperature region E-44 and E-7 have about the same t_0; this is because E-44 has a higher Δn than E-7, but its γ_1/K_{11} is also higher. As the temperature increases, t_0 of both materials decreases—however, at a different rate. The t_0 of E-7 decreases at a slower rate and saturates at a lower temperature (about 41°C). However, the t_0 of E-44 continues to improve before the optimal temperature ($T_{op} \approx 80$°C) is reached. Another interesting phenomenon occurs in RO-TN-404. Its t_0 at room temperature is about 50 per cent slower than that of E-44 because RO-TN-404 has a very high viscosity. Nevertheless, this difference becomes smaller as the temperature increases. At $T \approx 84$°C, the optimal temperature of RO-TN-404, its t_0 ($\approx 800\,\mu$s) is comparable (about 10 per cent slower) with that of E-44 (at $T_{op} \approx 80$°C).

From this example, the temperature effect on liquid-crystal performance is heavily dependent on T_{NI} and nematic range. The temperature range of a liquid-crystal mixture is determined by the compositions formulated. The major component of E-7, E-44 and RO-TN-404 is a cyanobiphenyl (5CB). 5CB has narrow nematic range (22·5–35·3°C). In order to expand the nematic range, some terphenyl (5CT) compound is added. Terphenyl has a very high melting point and a very wide nematic range (131–240°C) [18]. In addition, it has a high birefringence and a high viscosity. Mixtures consisting of biphenyls and terphenyl usually exhibit a wide nematic range, high birefringence and a high viscosity at room temperature. Higher T_{NI} (i.e. higher T_{op}) and a wide nematic range enable a mixture to reduce its viscoelastic coefficient to a greater extent, while the birefringence drop is moderate. This is the reason why E-44 and RO-TN-404 have higher merit factors than E-7 at their optimal temperatures.

(b) I.R. properties

Since E-44 has a great potential for I.R. applications, its I.R. absorption was measured by a spectrometer (2·5–50 μm), and the result is shown in figure 4 (*a*). Owing

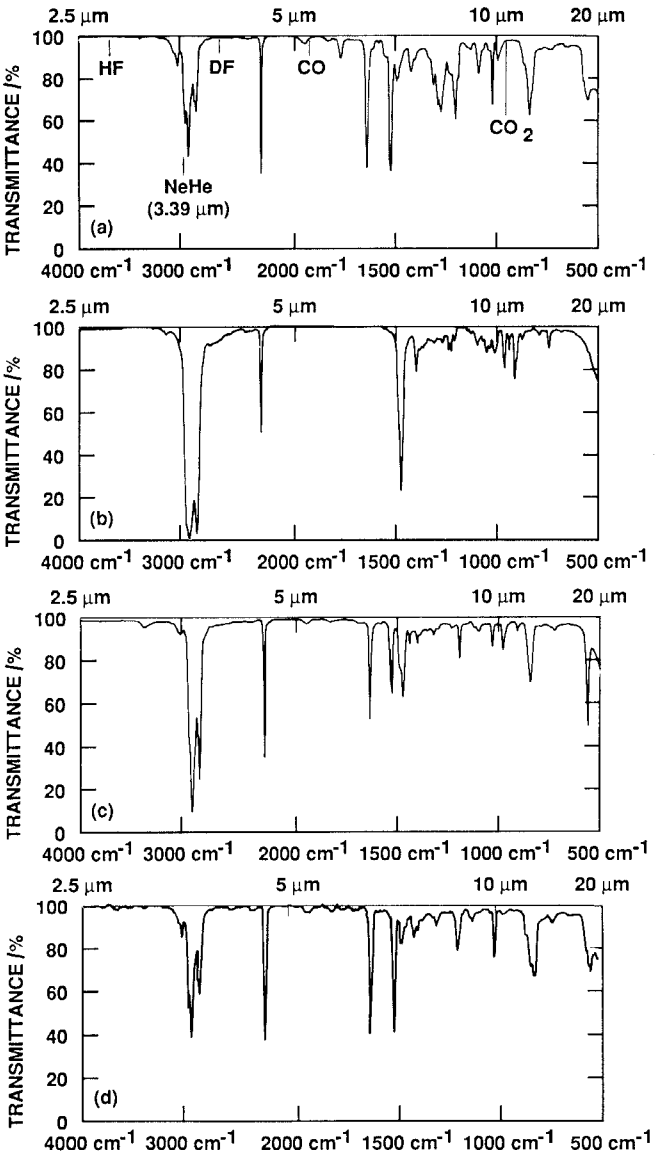

Figure 4. I.R. absorption spectra of (*a*) E-44 LC mixture, (*b*) CCH3 at $T \approx 50°C$, (*c*) PCH7, and (*d*) 5CB. Unpolarized light was used for the measurements. In (*a*) some I.R. laser lines are indicated. The truncation beyond $\lambda \approx 19\,\mu m$ is due to the KCl substrate absorption, not to the liquid crystal. The layer thickness used for each measurement was about $5\,\mu m$, but it was not controlled precisely. Apart from (*b*), all the other materials were studied at room temperature.

to the potassium chloride substrates used, wavelengths longer than about $19\,\mu m$ are truncated by the substrate absorption. From figure 4(*a*), although some molecular vibrational bands exist, there are some transparent windows, so that useful electro-optic applications can still be achieved. Also indicated in figure 4(*a*) are some I.R. laser lines. Except for the $3{\cdot}39\,\mu m$ HeNe laser line, E-44 is relatively transparent to many laser lines (including near-I.R. lasers).

In the interest of formulating a mixture for I.R. application, absorptions of three commercial pure compounds were also measured, and the results are shown in figures 4 (*b*), (*c*) and (*d*) for cyanocyclocyclohexane (CCH), cyanophenylcyclohexane (PCH) and cyanobiphenyl respectively. By comparing the absorption spectra as shown in figures 4 (*b*), (*c*) and (*d*), we are able to identify the origin of some vibrational bands. A more detailed assignment of these absorption bands can be found in [19]. It should be noted that CCH has a strong absorption band at the 10·6 μm CO_2 laser wavelength, therefore, when a mixture is considered for use at $\lambda = 10{\cdot}6\,\mu$m, CCH should be avoided.

4. Conclusion

Short-chain cyanotolanes and E-44 LC mixtures have shown some attractive features and are suitable for I.R. applications. Mixtures of cyanotolanes to lower and widen their nematic temperature remain to be investigated. Mesogenic molecules with longer conjugation length need to be synthesized. It is anticipated that highly conjugated molecules should show very high birefringence in both visible and I.R. regions. However, these molecules may have high melting points. Continuing to extent the π-electron conjugation may also encounter a thermodynamic stability problem. Therefore an optimal conjugation length may exist. Molecular design and synthesis will play a crucial role in achieving these optimal mesogenic molecules.

The authors are grateful to E. Ramos for her assistance in U.V. measurements on the cyanotolanes.

References

[1] Wu, S. T., Efron, U., and Hess, L. D., 1984, *Appl. Phys. Lett.*, **44**, 1033.
[2] Wu, S. T., 1986, *Phys. Rev.* A, **33**, 1270.
[3] Wu, S. T., Efron, U., Grinberg, J., Hess, L. D., and Welkowsky, M. S., 1985, *Proc. SPIE*, **672**, 94.
[4] Wu, S. T., 1988, *U.S. Patent* 4 762 399 and 4 768 864. Also Wu, S. T., 1986, *Proc. SPIE*, **684**, 108.
[5] Khoo, I. C., Michael, R. R., and Finn, G. M., 1988, *Appl. Phys. Lett.*, **52**, 2108.
[6] Sanchez, F., Kayoun, P. H., and Huignard, J. P., 1988, *J. appl. Phys.*, **64**, 26.
[7] Wu, S. T., Lackner, A. M., and Efron, U., 1987, *Appl. Optics*, **26**, 3441.
[8] Grinberg, J., Jacobson, A., Bleha, W. P., Miller, L., Fraas, L., Bosewell, D., and Myer, G., 1975, *Opt. Engng*, **14**, 217.
[9] Efron, U., Grinberg, J., Braatz, P. O., Little, M. J., Reif, P. G., and Schwartz, R. N., 1985, *J. appl. Phys.*, **57**, 1356.
[10] Wu, S. T., and Cox, R. J., 1988, *J. appl. Phys.*, **64**, 821.
[11] Wu, S. T., 1988, *J. appl. Phys.*, **64**, 815.
[12] Gray, G. W., and Mosley, A., 1976, *Molec. Crystals. liq. Crystals*, **37**, 213.
[13] Cox, R. J., and Clecak, N. J., 1976, *Molec. Crystals liq. Crystals*, **37**, 241.
[14] Aver'yanov, E. M., Zhuikov, V. A., Ya Zyryanov, V., and Shabanov, V. F., 1984, *Soviet Phys. JETP*, **59**, 1227.
[15] Wu, S. T., and Ramos, E., *Proc. SPIE on "Liquid Crystal Chemistry, Physics and Applications"*, edited by Z. Yaniv and J. W. Doane (in the press).
[16] Wu, S. T., and Wu, C. S., 1988, *Appl. Phys. Lett.*, **53**, 1794.
[17] Wu, S. T., and Wu, C. S., 1989, *J. appl. Phys.*, **65**, 527.
[18] Gray, G. W., 1975, *J. Phys., Paris*, **36**, 337.
[19] Rajalakshmi, P. K., Shivaprakash, N. C., and Prasad, J. S., 1980, *Molec. Crystals liq. Crystals*, **60**, 319.